AIAA JOURNAL
Vol. 38, No. 11, November 2000

Technical Notes

TECHNICAL NOTES are short manuscripts describing new developments or important results of a preliminary nature. These Notes cannot exceed six manuscript pages and three figures; a page of text may be substituted for a figure and vice versa. After informal review by the editors, they may be published within a few months of the date of receipt. Style requirements are the same as for regular contributions (see inside back cover).

Nonlinear Stress–Strain Model Accounting for Dissipation Anisotropies

Marcus C. Johansson,* Jens Knoell,† and Dale B. Taulbee‡
State University of New York at Buffalo, Buffalo, New York 14260

Introduction

WHEN the Reynolds stress transport equation is modeled, it is often assumed that the transport effects have minor significance. A second simplification includes an isotropic model for the dissipation rate tensor. However, numerical experiments on homogeneous turbulent shear flows indicate that the anisotropies in the dissipation rate tensor are sometimes one-half as large as the Reynolds stress anisotropies and are, therefore, not negligible.[1] In the present study, the importance of capturing anisotropic dissipation effects along with the transport of the Reynolds stresses for a successful algebraic Reynolds stress closure will be investigated utilizing the direct numerical simulation (DNS) data by Kim et al.[2] for a fully developed channel flow. On the basis of a two-dimensional explicit nonlinear stress–strain relation,[3] which represents a solution to the implicit algebraic Reynolds stress model (ARSM) for near-wall flows, an improved model is suggested using the observations made from the aforementioned investigation.

Model Derivation

The incompressible Reynolds stress transport equation can be written in terms of the Reynolds stress anisotropies a_{ij} and reads[4]

$$k\frac{\mathrm{D}a_{ij}}{\mathrm{D}t} = \underbrace{\frac{\partial T_{ijk}}{\partial x_k} - \frac{\overline{u_i u_j}}{k}\frac{\partial T_l}{\partial x_l}}_{A_{ij}} \underbrace{- \frac{\overline{u_i u_j}}{k}(P-\epsilon) + P_{ij} + \Phi_{ij} - \frac{2}{3}\epsilon\delta_{ij}}_{B_{ij}} \underbrace{- \left(\epsilon_{ij} - \frac{2}{3}\epsilon\delta_{ij}\right)}_{C_{ij}} \tag{1}$$

where $T_{ijk} = -\overline{u_i u_j u_k} - \overline{pu_j}\delta_{ik} - \overline{pu_i}\delta_{jk} + \nu\partial\overline{u_i u_j}/\partial x_k$ is the total transport of Reynolds stresses, $P_{ij} = -\overline{u_i u_k}\partial U_j/\partial x_k - \overline{u_j u_k}\partial U_i/\partial x_k$ the production tensor, $\Phi_{ij} = \overline{p(\partial u_i/\partial x_j + \partial u_j/\partial x_i)}$ the pressure–strain (PS) correlation, and $\epsilon_{ij} = 2\nu\overline{\partial u_i/\partial x_k\,\partial u_j/\partial x_k}$ the dissipation rate tensor. A_{ij}, B_{ij}, and C_{ij} are introduced to investigate the effects of the underlying model assumptions.

To close Eq. (1), the dissipation rate tensor can be modeled in an isotropic way as $\epsilon_{ij} = 2\delta_{ij}\epsilon/3$. In the context of explicit ARSMs the model for the PS is restricted to linear expansions, for example,

$$\Phi_{ij} = C_0 k S_{ij} - C_1\epsilon a_{ij} + (1-C_3)k(a_{ik}S_{kj} + a_{jk}S_{ki} - 2a_{mn}S_{mn}\delta_{ij}/3) - (1-C_4)k(a_{ik}\Omega_{kj} - a_{jk}\Omega_{ki}) \tag{2}$$

where k is the turbulent kinetic energy and ϵ the scalar dissipation. The terms S_{ij} and Ω_{ij} are the mean strain and rotation rate, respectively. To account for wall effects on the PS correlation, one approach is to adjust the PS coefficients.[3] The wall-modified PS coefficients can then be given as $C_i = C_{io} + C_{iw}f_w$ ($i = 0, 1, 3, 4$) with $f_w = \exp[k^+/(60\epsilon^+)]$. The constants C_{io} describe the wall-independent PS effects, and their calibration in the original model[3] is carried out for wall-independent homogeneous shear flows and for the equilibrium region of fully developed channel flows. The resulting values are $C_{0o} = 0.8$, $C_{1o} = 1.47$, $C_{3o} = 0.19$, and $C_{4o} = 0.41$.

Using the models for the dissipation rate tensor and the PS and neglecting the total transport effects A_{ij} as well as the convective term[4,5] yields the implicit ARSM:

$$-(\overline{u_i u_j}/k)(P-\epsilon) + P_{ij} + \Phi_{ij} - \tfrac{2}{3}\epsilon\delta_{ij} = 0 \tag{3}$$

This equation allows an explicit solution,[6] which can be used as a two-dimensional stress–strain relation applicable in two-equation models:

$$a_{ij} = -2C_\mu\left[\tau S_{ij} - C_3 g\tau^2 S_{nm}S_{nm}\left(\delta_{ij}^{(2)} - \tfrac{2}{3}\delta_{ij}^{(3)}\right) + C_4 g\tau^2(S_{ik}\Omega_{kj} + S_{jk}\Omega_{ki})\right]$$

$$C_\mu = \frac{\frac{1}{2}\left[\left(\frac{4}{3} - C_0\right)g\right]}{1 - \frac{2}{3}C_3^2 g^2\tau^2 S_{nm}S_{nm} + 2C_4^2 g^2\tau^2\Omega_{nm}\Omega_{nm}}$$

$$g = \frac{1}{C_1 - 1 + P/\epsilon}, \qquad \tau = \frac{k}{\epsilon} \tag{4}$$

The wall-dependent PS constants C_{iw} are calibrated against the wall region of a channel flow and a turbulent boundary layer by optimizing the resulting mean velocity and the Reynolds shear stress for the final model. The values read $C_{0w} = 0.21$, $C_{1w} = 0.47$, $C_{3w} = 0.71$, and $C_{4w} = 0.27$. The resulting model leads to fair predictions for the Reynolds stress anisotropies. However, it is hypothesized that a term-by-term representation of the Reynolds stress budget, also including a model for the dissipation anisotropies, can further improve the results.

In Eq. (1) B_{ij} corresponds to the terms accounted for in the ARSM. The term C_{ij} stands for the dissipation anisotropies. To analyze the Reynolds stress anisotropy budgets, DNS data[2] for a two-dimensional fully developed channel flow at $Re_\tau = 395$ are investigated. Here, the convective term $\mathrm{D}a_{ij}/\mathrm{D}t$ is identically zero. Figure 1a shows the anisotropy budget of the normal component in the streamwise direction a_{11}. It is clear that the ARSM term B_{11} and the dissipation anisotropies C_{11} dominate the budget compared to the transport effects A_{11}. In the other normal directions, a similar trend is apparent, and, therefore, the plots are omitted. The shear budget is shown in Fig. 1b. Here, the transport term A_{12} plays an important role together with the ARSM term B_{12}. The role of the dissipation anisotropy C_{12} appears to be of minor importance except very close to the wall. Because an explicit stress–strain relation

Received 4 May 2000; accepted for publication 14 June 2000. Copyright © 2000 by the American Institute of Aeronautics and Astronautics, Inc. All rights reserved.

*Graduate Student, Department of Mechanical and Aerospace Engineering.
†Research Assistant, Department of Mechanical and Aerospace Engineering.
‡Professor, Department of Mechanical and Aerospace Engineering; trldale@eng.buffalo.edu.

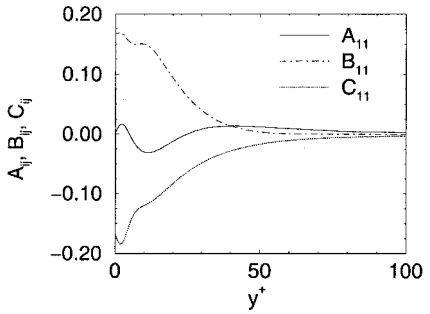

Fig. 1a Budget for a_{11}.

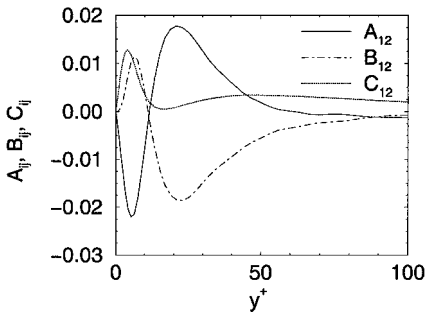

Fig. 1b Budget for a_{12}.

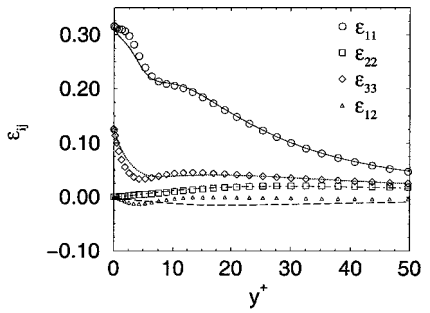

Fig. 1c Components of the dissipation tensor ϵ_{ij}.

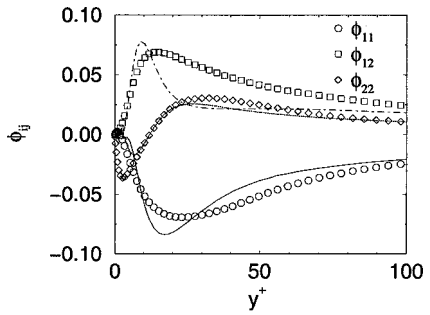

Fig. 1d Φ_{ij}, symbols, DNS data,[2] lines, and model predictions.

based on the solution to the implicit ARSM is desired, the expression for ϵ_{ij} has to be linear in the Reynolds stresses. The model used in the present study is based the following proposal by Hanjalić and Jakirlić[7]:

$$\epsilon_{ij} = \epsilon\left[\left(1 - f_s^{\epsilon}\right)\tfrac{2}{3}\delta_{ij} + \left(\overline{u_i u_j}/k\right) f_s^{\epsilon}\right] \tag{5}$$

This formulation assumes a proportionality between the large-scale anisotropies of the Reynolds stresses and the small-scale dissipation anisotropies in the vicinity of the wall. Farther away from the wall, ϵ_{ij} reaches the isotropic limit. In contrast to the original suggestion,[7] f_s^{ϵ} is chosen to be a function of the turbulent timescale τ as $f_s^{\epsilon} = \exp(-\tau^+/300)$. This function is optimized against the channel flow DNS data at $Re_\tau = 395$. Figure 1c shows the performance of the anisotropic dissipation model. Whereas the normal components of ϵ_{ij} are represented with high accuracy, the shear component fails to capture the characteristics in the near-wall region.

Because a term-by-term modeling strategy of the Reynolds stress transport equation is desired, the wall-dependent PS constants C_{iw}, appearing in the PS model, are now calibrated directly against the PS data from the DNS. The resulting new set of coefficients reads $C_{0w,n} = -1.86$, $C_{1w,n} = 1.47$, $C_{3w,n} = 0.97$, and $C_{4w,n} = 1.27$. The model predictions compared the DNS pressure strain are shown in Fig. 1d. The modeled PS in the streamwise direction Φ_{11}, together with the PS model in the wall-normal direction Φ_{22}, show fair agreement with the DNS data. The shear component, however, lacks accuracy in the buffer layer of the channel flow.

From the preceding investigation it can be seen that the models adopted for the PS and the dissipation rate tensor yield inaccurate results in the shear direction. Moreover, it can be concluded that the difference between the two transport terms for the shear component is not negligible. Recently, Ni[8] proposed a model accounting for the transport terms and allowing the application in two-equation models. However, the latter model is computationally cumbersome to handle because it requires third derivatives of the mean velocity. On the other hand, without a representation of A_{12}, the Reynolds stress budget in the shear direction cannot be balanced. This dilemma leads to a proposition of a composite model consisting of different sets of wall-dependent PS coefficients for the shear and normal components of the Reynolds stresses. The stress–strain model with the original PS[3] coefficients predicts $\overline{uv}$ very well for the considered test case because the calibration procedure causes the PS model to account also for the dissipation anisotropies and the transport terms in the shear direction. Thus, the original proposal in Eq. (4) is used in the shear direction. For the normal components, the transport term is negligible, and the dissipation anisotropies can be well captured with the new model for ϵ_{ij}. Therefore, a term-by-term representation of the normal Reynolds stress transport equation is appropriate, and the newly calibrated wall-dependent PS coefficients $C_{iw,n}$ are used together with the calibrated model for the dissipation anisotropies. Solving this extended ARSM for the normal directions yields the

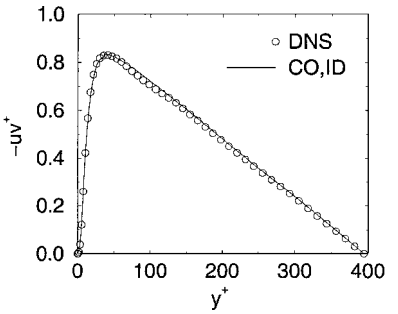

Fig. 2a Reynolds shear stress.

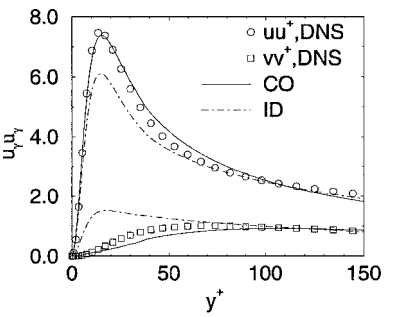

Fig. 2b Reynolds normal stresses, symbols, DNS data,[2] lines, and model predictions.

following explicit stress–strain expressions for $a_{\gamma\gamma}$ (no summation over γ):

$$a_{\gamma\gamma} = -2C_{\mu,n}\Big[\tau S_{ij} - C_{3,n} g_n \tau^2 S_{nm} S_{nm}\left(\delta_{ij}^{(2)} - \tfrac{2}{3}\delta_{ij}^{(3)}\right) + C_{4,n} g_n \tau^2 (S_{ik}\Omega_{kj} + S_{jk}\Omega_{ki})\Big]$$

$$C_{\mu,n} = \frac{\frac{1}{2}\left(\frac{4}{3} - C_{0,n}\right) g_n}{1 - \frac{2}{3}C_{3,n}^2 g_n^2 \tau^2 S_{lm} S_{lm} + 2C_{4,n}^2 g_n^2 \tau^2 \Omega_{lm}\Omega_{lm}}$$

$$g_n = \frac{1}{C_{1,n} - 1 + P/\epsilon + f_s^{\epsilon}} \tag{6}$$

The corresponding k–ϵ model is based on the formulation by Hanjalić and Launder,[9] but includes a second source term for ϵ and the use a modified timescale. Details are given in Ref. 3.

Results

In Figs. 2a and 2b, the Reynolds stress results for the newly proposed composite model (CO) are compared to results of the original model with an isotropic dissipation (ID) and DNS data for a channel flow.[2] Because the CO and the ID models both use the same expression to calculate $\overline{uv}$, the profiles are identical. The predictions are in good agreement with the DNS data. For the normal components of $\overline{u_i u_j}$ the CO model leads to improved predictions compared to the ID model as can be seen in the examples for $\overline{uu}$ and $\overline{vv}$. Predictions of the CO model for a channel flow case at $Re_\tau = 180$ show similar features as for the high-Reynolds-number case and are, therefore, not elaborated on in this Note.

Conclusions

It is shown that a more accurate prediction of the normal stresses in the near-wall region requires an anisotropic dissipation model. Because of the lack of a model for the transport terms, which allows the explicit solution of the ARSM, these effects are often discarded. In this Note, however, it is shown that the latter assumption is not permissible in the shear direction. Hence, a new composite model formulation is presented remedying some of the previous inconsistencies. As a result, the new composite model shows improvements in modeling the normal stresses for a channel flow compared to the basic model and, therefore, promotes further studies in this direction.

References

[1]Durbin, P. A., and Speziale, C. G., "Local Anisotropy in Strained Turbulence at High Reynolds Numbers," *Journal of Fluids Engineering,* Vol. 113, No. 4, 1991, pp. 707–709.

[2]Kim, J., Moin, P., and Moser, R., "Turbulence Statistics in Fully Developed Channel Flow at Low Reynolds Number," *Journal of Fluid Mechanics,* Vol. 177, 1987, pp. 133–166.

[3]Knoell, J., and Taulbee, D. B., "A Nonlinear Stress-Strain Model for Wall-Bounded Turbulent Flows," *Engineering Turbulence Modeling and Measurements 4,* edited by W. Rodi and D. Laurence, Elsevier Science, Oxford, 1999, pp. 103–112.

[4]Taulbee, D. B., "An Improved Algebraic Reynolds Stress Model and Corresponding Nonlinear Stress Model," *Physics of Fluids A,* Vol. 4, No. 11, 1992, pp. 2555–2561.

[5]Rodi, W., "A New Algebraic Relation for Calculating the Reynolds Stresses," *ZAMM,* Vol. 56, No. 3, 1976, pp. T219–T221.

[6]Pope, S. B., "A More General Effective-Viscosity Hypothesis," *Journal of Fluid Mechanics,* Vol. 72, No. 2, 1975, pp. 331–340.

[7]Hanjalić, K., and Jakirlić, S., "A Model of Stress Dissipation in Second-Moment Closures," *Applied Scientific Research,* Vol. 51, 1993, pp. 513–518.

[8]Ni, W., "Nonlinear Eddy-Viscosity Turbulence Model and Its Application," *AIAA Journal,* Vol. 37, No. 8, 1999, pp. 1000–1002.

[9]Hanjalić, K., and Launder, B. E., "A Reynolds Stress Model of Turbulence and Its Application to Thin Shear Flows," *Journal of Fluid Mechanics,* Vol. 52, No. 4, 1972, pp. 609–638.

J. P. Gore
Associate Editor

Direct Circulation Measurement of a Tip Vortex

K. J. Desabrais* and H. Johari†
Worcester Polytechnic Institute, Worcester, Massachusetts 01609

Introduction

THE circulation of tip vortices has traditionally been calculated by taking the line integral of the velocity around a closed path surrounding the vortex, which requires detailed knowledge of the velocity field. Measurements of the velocity field can be made by either single-point anemometry or whole-field particle image velocimetry (PIV) techniques. Alternatively, if vortex circulation is the primary parameter of interest, the direct measurement of circulation can be achieved via acoustic means, thus eliminating the need for detailed velocity measurements. An acoustic method that allows for a simple, nonintrusive method of circulation measurement has been developed in our laboratory utilizing narrow ultrasound beams.[1] This method significantly decreases the time it takes to find the circulation in a specified region of the flow. The method has been used to measure the circulation of delta wing vortices[2] and the bound circulation of an airfoil.[1] This method was utilized in the current study to examine the circulation of a tip vortex.

Tip vortices have been studied extensively in the past. Most of the studies have examined the behavior of vortices using classical anemometry techniques.[3–6] More recently, PIV has been employed to obtain detailed velocity field measurements of the tip vortex in the near field[7] and the far field.[8] Various vortex characteristics such as circulation have been extracted from these velocity fields. The vortex circulation measured by our ultrasound method is compared against previous data to assess the applicability of the ultrasound technique.

Ultrasound Method

The ultrasound technique is based on the time of flight of sound pulses traversing a given path. Sound travels through fluids with a velocity that is the sum of the local sound speed and the local flow velocity. If the local flow velocity augments (retards) the sound speed, the time of flight would be decreased (increased). In our setup, a sound pulse was transmitted around a closed rectangular path in one direction, and its transit time was accurately measured. The process was then repeated by emitting a pulse in the opposite direction around the closed path. In the presence of a vortex, a time difference Δt would be generated from transversing the path in opposite directions. As derived by Johari and Durgin,[1] the net circulation Γ is linearly proportional to the time difference, that is, $\Gamma = \frac{1}{2}a^2\Delta t$, as long as the sound speed a is constant along the path during the transit time and the velocity component along the acoustic path is small, for example, less than $0.1a$. Further details of the method, its advantages, and limitations are discussed by Johari and Durgin.[1]

Experimental Setup

The experiments were conducted in the Worcester Polytechnic Institute low-speed wind tunnel that has test section dimensions of 45.7 cm high × 61.0 cm wide × 91.4 cm long. To create a tip vortex, a half-wing was mounted vertically from the tunnel ceiling. The wing was a blunt-ended, rectangular planform NACA 0012 with a chord c of 10.5 cm and a semispan s of 22.3 cm resulting in a (half-wing) aspect ratio of 2.1. The angle of attack was measured

Received 16 August 1999; revision received 6 July 2000; accepted for publication 21 July 2000. Copyright © 2000 by K. J. Desabrais and H. Johari. Published by the American Institute of Aeronautics and Astronautics, Inc., with permission.

*Graduate Student, Mechanical Engineering Department. Student Member AIAA.

†Associate Professor, Mechanical Engineering Department. Senior Member AIAA.